

An Adaptive Neuro - Fuzzy Approach to Estimate Electric and Magnetic Fields Around Iraqi 132kV Power Transmission Lines

Lect. Dr. Suad Ibrahim
Electrical and Electronic Eng. Dept.
University of Technology
Baghdad- Iraq

Asst. Lect. Fadhil Abbas Hassan
Electrical and Electronic Eng.
Dept University of Technology,
Baghdad, Iraq

Abstract

This research presents an approach based on the adaptive neuro-fuzzy inference system (ANFIS) to estimate electric and magnetic fields around Iraqi 132kV transmission lines. This system has been trained, using finite element calculations for three cases study having different span locations crossing of public services (roads, buildings). It is proved that proposed approach may be used to calculate the electromagnetic fields in new cases differing significantly from the cases used for training with the high accuracy and time efficiency.

الخلاصة

يقدم هذا البحث طريقة مستندة على النظام الضبابي العصبي التكيفي (ANFIS) لتخمين المجالات الكهربائية والمغناطيسية من حول خطوط نقل الطاقة 132kV. درب هذا النظام باستخدام حسابات العنصر المحدود وثلاثة حالات دراسية عند مواقع مختلفة للـ (span) عبر الخدمات الحكومية (طرق, بنايات). وقد أثبت ان الطريقة المقترحة قد تستخدم لحساب المجالات الكهرومغناطيسية في الحالات الجديدة والتي تختلف بشكل ملحوظ عن الحالات التي استعملت للتدريب وبدقة عالية وكفاءة زمنية.

1. Introduction

The use of finite element method (FEM) for the solution of Maxwell's differential equations describing an electromagnetic field problem always leads to useful conclusions [1,2]. However, the complicated geometries of complex electromagnetic field problems leads to a large number of discretization nodes and consequently to a huge computational effort. Therefore, a scaling method of the results from one configuration case to another may be of interest if it needs shorter computing time than an additional FEM calculation. Fuzzy logic, which is a research area of artificial intelligence (AI), seems to be an efficient method to create systems capable of learning relationships and using this knowledge for further calculations.

Several attempts have been done in order to quickly estimate the electromagnetic field problem. In [3, 4] Takagi-Sugeno fuzzy system is used to determine the magnetic field induced by a faulted transmission line on a buried pipeline. The genetic algorithm has been developed for the adjustment of the fuzzy parameters. Artificial neural networks also are used for estimating electromagnetic field, [5, 6]. ANFIS has been successfully applied to a number of engineering problems during recent years.

In [7] is presented architecture and learning procedure of this fuzzy inference system implemented in the framework of adaptive networks. One of ANFIS applications is modeling complex nonlinear functions by a set of fuzzy rules. Neural network and fuzzy logic system are universal approximates.

This work presents an approach based on the use ANFIS to estimate electric and magnetic fields around Iraqi 132kV overhead power transmission line in case study for two configurations (flat and vertical) and different span locations crossing of public services (normal ground, main roads, buildings). Two ANFIS are trained using hybrid learning algorithm. The output of the first ANFIS is intensity of electric field E , while the output of the second neural network is magnetic field B . Computer simulation is applied finite element method in the time harmonic mode that is developed by ANSYS software environment, the model results are used for training of ANFIS.

2. Numerical Model

In the low-frequency region, the electromagnetic wavelength is much larger than the dimensions of the computational domain such that wave propagation phenomena can be neglected. Consequently, the electromagnetic fields are described by quasi-static Maxwell's equations. The quasi-static approximation allows the assumption that only one field is dominant and thus it is possible to de-couple the electric and magnetic relations and only consider the dominant field [8].

2.1 Finite Element Formulation

When no magnetic excitation is present, the induced currents can be neglected with respect to the conductive and the dielectric currents, resulting in the so-called electroquasistatic. With the $\nabla \times E = 0$. In this case, the electric field strength E is curl-free: approach^[9]. assumption of no electric charges in the computational domain, the displacement current D is The electric field contains no rotational components. Hence, it can $\nabla \cdot D = 0$ divergence free: be expressed by the gradient of the electric scalar potential V as

$$E = -\nabla V \tag{1}$$

Inserting (1) into Ampère's law yields

$$\nabla \times H = J + \frac{\partial D}{\partial t} = \sigma E + \varepsilon \frac{\partial E}{\partial t} = -(\sigma \nabla V) - \left(\varepsilon \nabla \frac{\partial V}{\partial t} \right) \tag{2}$$

Where ε is permittivity of the medium and σ is the electrical conductivity. Because of the, the left application of the divergence operator $\nabla \cdot (\nabla \times) = 0$ general vector-analytic property on (2) leads to the complex-valued div-grad equation

$$-\nabla \cdot (\sigma \nabla V) - \nabla \cdot \left(\varepsilon \nabla \frac{\partial V}{\partial t} \right) = 0 \tag{3}$$

In a similar fashion, the magnetic field B may be expressed as a magnetic vector potential A , that is defined by^[10]:

$$B = \mu H = \nabla \times A : \nabla \cdot A = 0 \tag{4}$$

The governing equations for vectors of magnetic field H and electric field E in a quasistatic system are:

$$\nabla \times H = J \tag{5}$$

$$\nabla \times E = -\frac{\partial B}{\partial t} \tag{6}$$

The electric field can be written in terms of the magnetic vector potential A and the electric scalar potential V as

$$E = -\nabla V - \frac{\partial A}{\partial t} \tag{7}$$

In the quasistatic limit, the divergence of the induced current density is zero and therefore

$$\nabla \cdot \left(-\nabla V - \frac{\partial A}{\partial t} \right) = 0 \tag{8}$$

The finite element method was used for the numerical solution of the vector potentials.

2.2 Boundary Conditions and Simulation Parameters

This research is to focus on a power transmission system in Iraq, especially double-circuit, 132-kV overhead power transmission line, vertical configuration using Twin ACSR “Teal” 2-bundled phase conductor (Overall diameter=25.25 mm) as illustrated diagrammatically by Figure 1. While overhead ground wires (OHGW) are ACSR 'Dorking' (Overall diameter = 16.02 mm) ^[11].

The boundary conditions applied here are that both electric and magnetic fields at the ground level and the OHGW are set as zero. In contrast, the boundary conditions at the conductor surfaces are practically different.

They are strongly dependent upon the load current for the magnetic case. However, in this paper, the boundary conditions of both electric and magnetic fields of conductor surfaces in 132-kV power lines are assigned as given in ^[12], under the maximum loading of 1000A/phase. This simulation uses the system frequency of 50 Hz.

The power lines are bared conductors of Aluminum Conductor Steel Reinforced (ACSR), having the conductivity (σ) = 0.8×10^7 S/m, the relative permeability (μ_r) = 300, the relative permittivity (ϵ_r) = 3.5. It notes that the free space permeability (μ_0) is $4\pi \times 10^{-7}$ H/m, and the free space permittivity (ϵ_0) is 8.854×10^{-12} F/m.

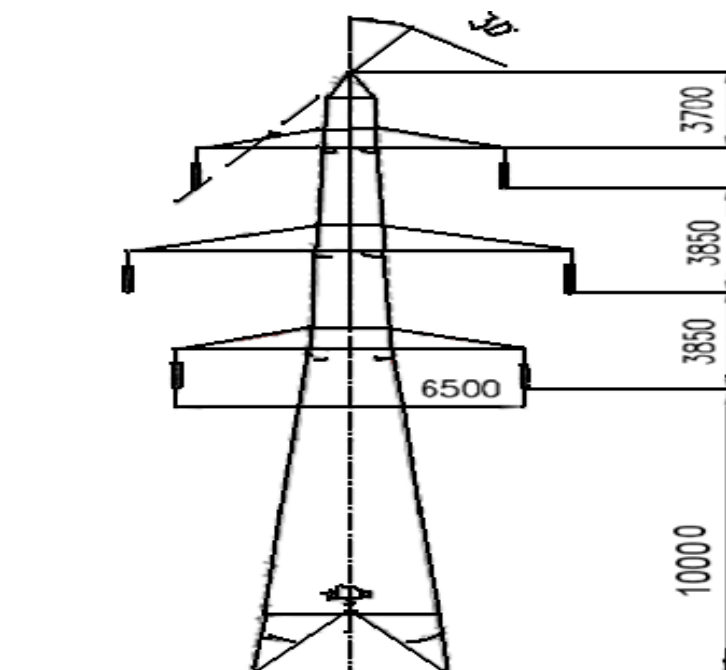


Figure (1) Cross- section of double circuit 132 kV transmission line with dimension (mm)

3. Adaptive Neuro-Fuzzy Inference System (ANFIS) Model

3.1 ANFIS Model Architecture and Operation

Suppose that Takagi-Sugeno fuzzy system has m inputs (x_1, x_2, \dots, x_m) and one output t . Linguistic labels x_i are $A_{1i}, A_{2i}, \dots, A_{ni}$. The rule base contains $p = n^m$ if-then rules:

$$R_1: \text{if } x_1 \text{ is } A_{11} \text{ and } x_2 \text{ is } A_{12} \dots \text{ and } x_m \text{ is } A_{1m} \text{ then} \\ f_1 = p_{11}x_1 + p_{12}x_2 + \dots + p_{1m}x_m + c_1$$

$$R_2: \text{if } x_1 \text{ is } A_{21} \text{ and } x_2 \text{ is } A_{22} \dots \text{ and } x_m \text{ is } A_{2m} \text{ then} \\ f_2 = p_{21}x_1 + p_{22}x_2 + \dots + p_{2m}x_m + c_2$$

...

$$R_k: \text{if } x_1 \text{ is } A_{k1} \text{ and } x_2 \text{ is } A_{k2} \dots \text{ and } x_m \text{ is } A_{km} \text{ then} \\ f_k = p_{k1}x_1 + p_{k2}x_2 + \dots + p_{km}x_m + c_k$$

...

$$R_p: \text{if } x_1 \text{ is } A_{p1} \text{ and } x_2 \text{ is } A_{p2} \dots \text{ and } x_m \text{ is } A_{pm} \text{ then} \\ f_p = p_{p1}x_1 + p_{p2}x_2 + \dots + p_{pm}x_m + c_p$$

The number of linguistic rules is $p = n^m$.

The equivalent ANFIS architecture ^[7, 13] (type-3 ANFIS) is shown in Figure 2.

Layer 1

The outputs of this layer are fuzzy membership grade of inputs $\mu_{A_{ij}}(x_j)$. If the bell shaped membership function is taken, $\mu_{A_{ij}}(x_j)$ is given by

$$\mu_{A_{ij}}(x_j) = \frac{1}{1 + \left[\left(\frac{x_j - a_{ij}}{c_{ij}} \right)^2 \right]^{b_{ij}}}, i = 1, n, j = 1, m \tag{9}$$

where: a_{ij}, b_{ij}, c_{ij} are the parameters of the membership function or premise parameters. The Gaussian membership function is given by:

$$\mu_{A_{ij}}(x_j) = e^{-\left(\frac{(c_{ij} - x_j)}{2\sigma_{ij}^2} \right)^2}, i = 1, n, j = 1, m \tag{10}$$

where: a_{ij}, σ_{ij} are the centre and width of the fuzzy set A_{ij}

Layer 2

Every node in this layer is a fixed node. The output of nodes can be presented as:

$$u_1 = \mu_{A_{11}}(x_1) * \mu_{A_{12}}(x_2) \cdots * \mu_{A_{1m}}(x_m)$$

$$u_2 = \mu_{A_{21}}(x_1) * \mu_{A_{22}}(x_2) \cdots * \mu_{A_{2m}}(x_m)$$

$$u_k = \mu_{A_{k1}}(x_1) * \mu_{A_{k2}}(x_2) \cdots * \mu_{A_{km}}(x_m)$$

$$u_p = \mu_{A_{p1}}(x_1) * \mu_{A_{p2}}(x_2) \cdots * \mu_{A_{pm}}(x_m)$$

* denotes *T*-norm. Nodes is marked by a circle and labeled Π.

Layer 3

The output of each fixed node label with N can be presented as:

$$\bar{u}_i = \frac{u_i}{\sum_{i=1}^p u_i} \tag{11}$$

Layer 4

Every node in this layer is a square. The outputs of this layer are given by:

$$\bar{u}_i f_i = \bar{u}_i \left(\sum_{j=1}^m p_{ij} x_j + c_i \right) \tag{12}$$

Layer 5

Finally, the output of the ANFIS can be presented as:

$$t = \frac{\sum_{i=1}^p \bar{u}_i f_i}{\sum_{i=1}^p u_i} = \frac{1}{\sum_{i=1}^p u_i} \sum_{i=1}^p u_i \left(\sum_{j=1}^m p_{ij} x_j + c_i \right) \tag{13}$$

In [7] the hybrid learning algorithm is used for updating the parameters. For adapting premise parameters a_{ij} , b_{ij} , c_{ij} gradient descent method is used. The least squares method is used for updating the consequent parameters.

The ANFIS is trained off-line using the training set $P = \{p_1, p_2, \dots, p_r\}$. Each element of the set, $p_k = (x_k, t_{zk})$ is defined by the input vector $x_k = (x_{1k} x_{2k} \dots x_{mk})$ and the desired response t_{zk} .

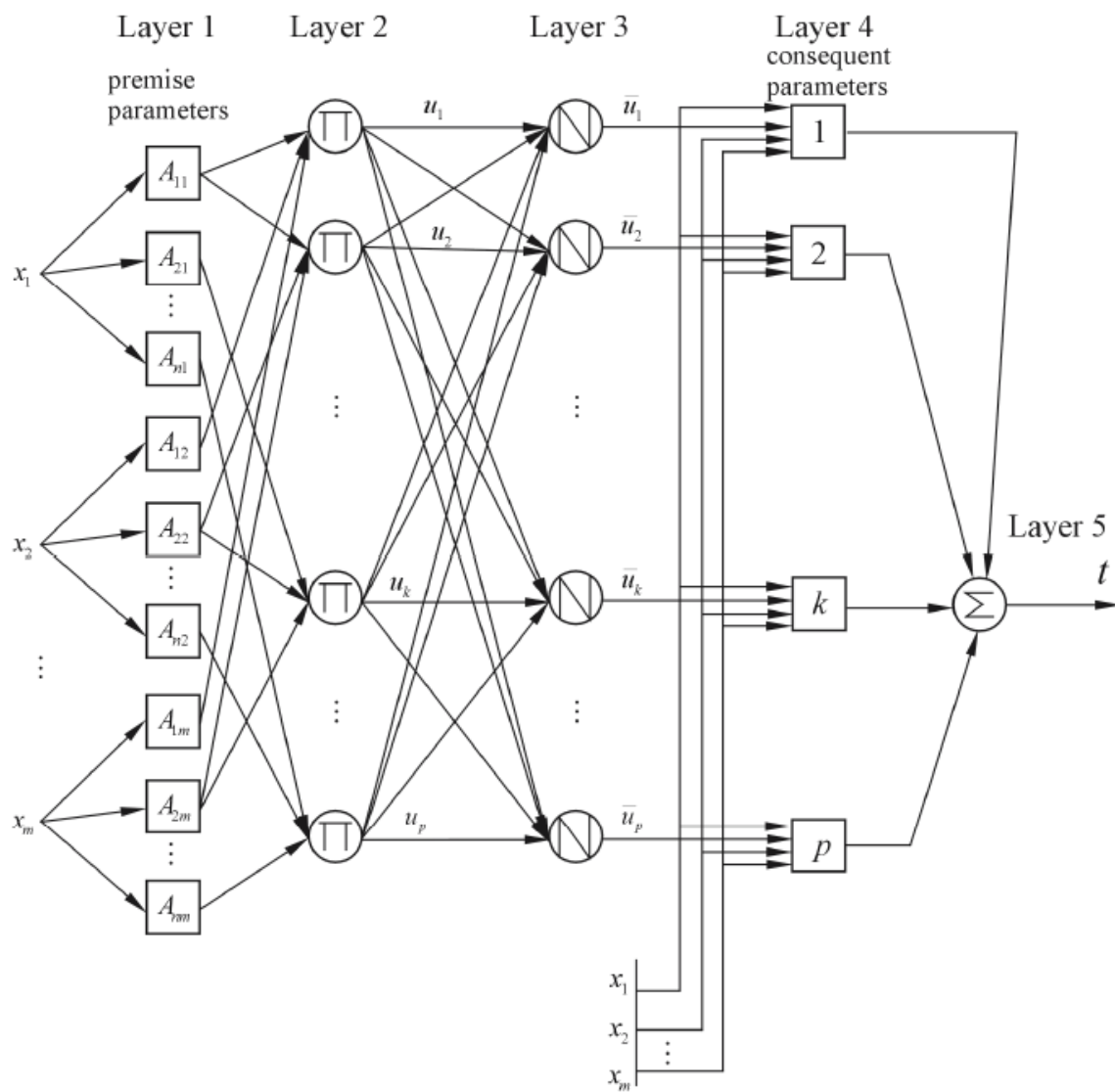


Figure (2) m -input ANFIS with p rules

In this work, a three-input single-output ANFIS has been used. The inputs and the output of the ANFIS are as follows:

Inputs: coordinate x (distance from center line in meter), coordinate y (height above ground level in meter) and coordinate h (clearance from conductor to ground) crossing of public services:

- i. Normal ground 7.5 meters
- ii. Main roads-road level 10 meters
- iii. Building or structure on which a man may stand 5 meters

Output: each of the two ANFIS has one output variable

Electric Field $E(kV/m)$ and Magnetic Flux Density $B(mG)$

ANFIS algorithms are implemented using the MATLAB fuzzy toolbox.

3.2 ANFIS Training

After the input selection process, FEM results of vertical configuration case of the system shown in Figure 1 are used to create a suitable training data base for the ANFIS using a hybrid learning algorithm. The training data set is the electric and magnetic fields (E and B) amplitude values for the different clearance crossing of public services ($h=5m, 7.5m, 10m$) with coordinates $x = (\text{from } 0m(\text{center line}) - \text{step } 2m - \text{ to } \pm 50m)$ and $y=(0m, 1m, 3m)$ above ground.

In Figure 3 is shown membership functions of input variables, h , x and y for electric field E and magnetic field B , after parameter adjustment using hybrid optimization procedure during ANFIS training process. Gaussian function was used as a membership function in the ANFIS model.

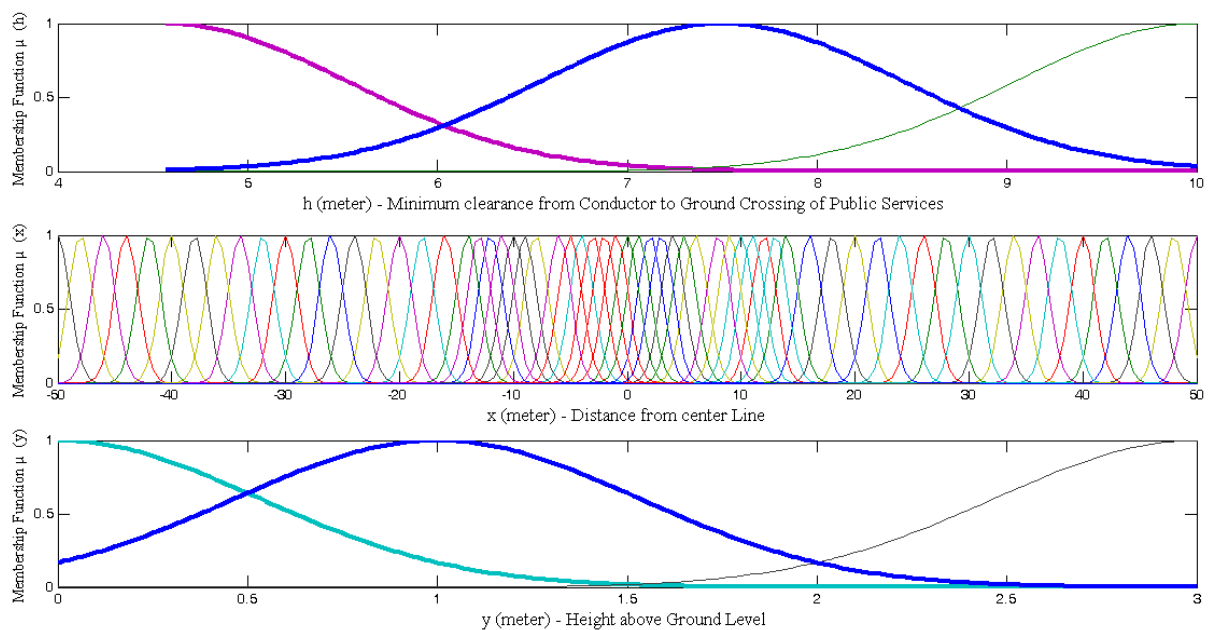


Figure (3) Memberships functions of input variables, h , x and y after training

4. Test Results

The method has been tested in two different cases; the first geometry is vertical configuration transmission line. Table 1 summarized test results are randomly chosen from different positions around 132kV transmission line where E and B calculations by the ANFIS and the FEM have been compared.

The absolute errors have been computed as:

$$e_E = \left| \frac{E_{FEM} - E_{ANFIS}}{E_{FEM}} * 100 \right| \quad \text{and} \quad e_B = \left| \frac{E_{FEM} - E_{ANFIS}}{E_{FEM}} * 100 \right|$$

For this case, the average absolute error between FEM and ANFIS is 0.3983% and 0.4212% for the examined electric field and magnetic field problems respectively.

Figure 4 and Figure 5 show horizontal profile of electric field and magnetic field as a function of the node's coordinate x in the air for the vertical configuration, as it is calculated by FEM and ANFIS. In both cases, ANFIS seems to follow satisfactory the results of FEM.

Table (1) Intensity electric field and magnetic field for different position cases of the examined electromagnetic field problem, obtained by the FEM and ANFIS

Clearance $h(m)$	Coordinates		FEM		ANFIS		$e_E(\%)$	$e_B(\%)$
	$x(m)$	$y(m)$	$E(kV/m)$	$B(mG)$	$E(kV/m)$	$B(mG)$		
5	3	0.5	1.8300	63.8430	1.8268	63.5079	0.1765	0.5249
5	13	0.5	0.0443	26.5300	0.0451	26.5867	1.9079	0.2137
5	25	0.5	0.0340	7.9878	0.0348	8.0051	0.0235	0.2167
5	11	2	0.3018	40.6820	0.3078	40.7313	1.9916	4.8588
5	17	2	0.0289	19.4310	0.0291	19.4921	0.3886	0.3143
5	33	2	0.0279	3.6222	0.0280	3.6280	0.0433	0.1608
7.5	5	0.5	1.2235	29.4810	1.2002	28.6869	1.9026	2.6935
7.5	15	0.5	0.1223	20.3210	0.1257	20.1934	2.7899	0.6282
7.5	29	0.5	0.0328	5.3832	0.0329	5.3929	0.0030	0.1804
7.5	9	2	0.5230	19.5370	0.5332	19.8639	1.9514	1.6733
7.5	21	2	0.0346	12.1540	0.0345	12.1791	0.0340	0.2068
7.5	35	2	0.0249	3.0724	0.0247	3.0769	0.0080	0.1459
10	1	0.5	1.233	25.5150	1.0181	25.3388	0.5118	0.6907
10	19	0.5	0.0693	11.5660	0.0696	11.5631	0.4269	0.0252
10	27	0.5	0.0425	6.2074	0.0426	6.2160	0.1132	0.1388
10	7	2	0.7013	13.0960	0.7018	13.2593	0.0723	1.2470
10	23	2	0.0473	8.7085	0.0474	8.7196	0.1556	0.1270
10	45	2	0.0150	1.4492	0.0152	1.4503	0.0133	0.0790

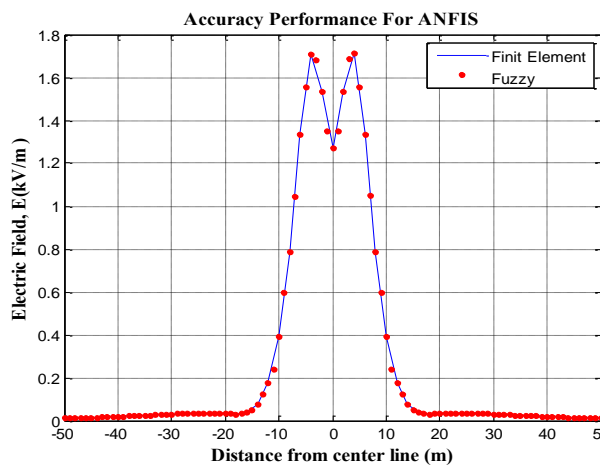


Figure (4) Electric field values on Horizontal profile of the vertical configuration calculations by FEM and ANFIS

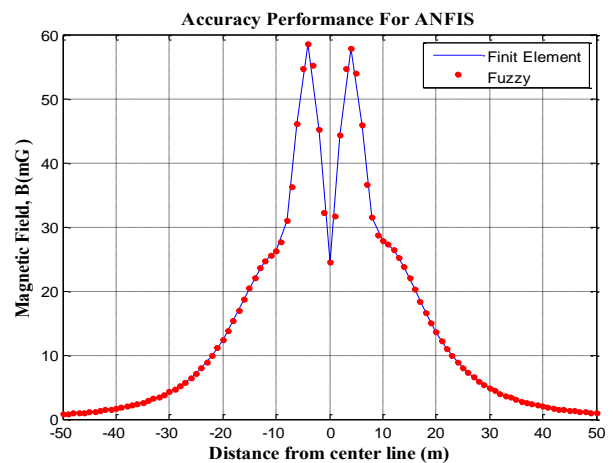


Figure (5) Magnetic field values on Horizontal profile of the vertical configuration calculations by FEM and ANFIS

Three-dimensional distribution of the electric and magnetic fields is obtained by the ANFIS is shown in Figure 6 and Figure 7 for three cases of span location charts.

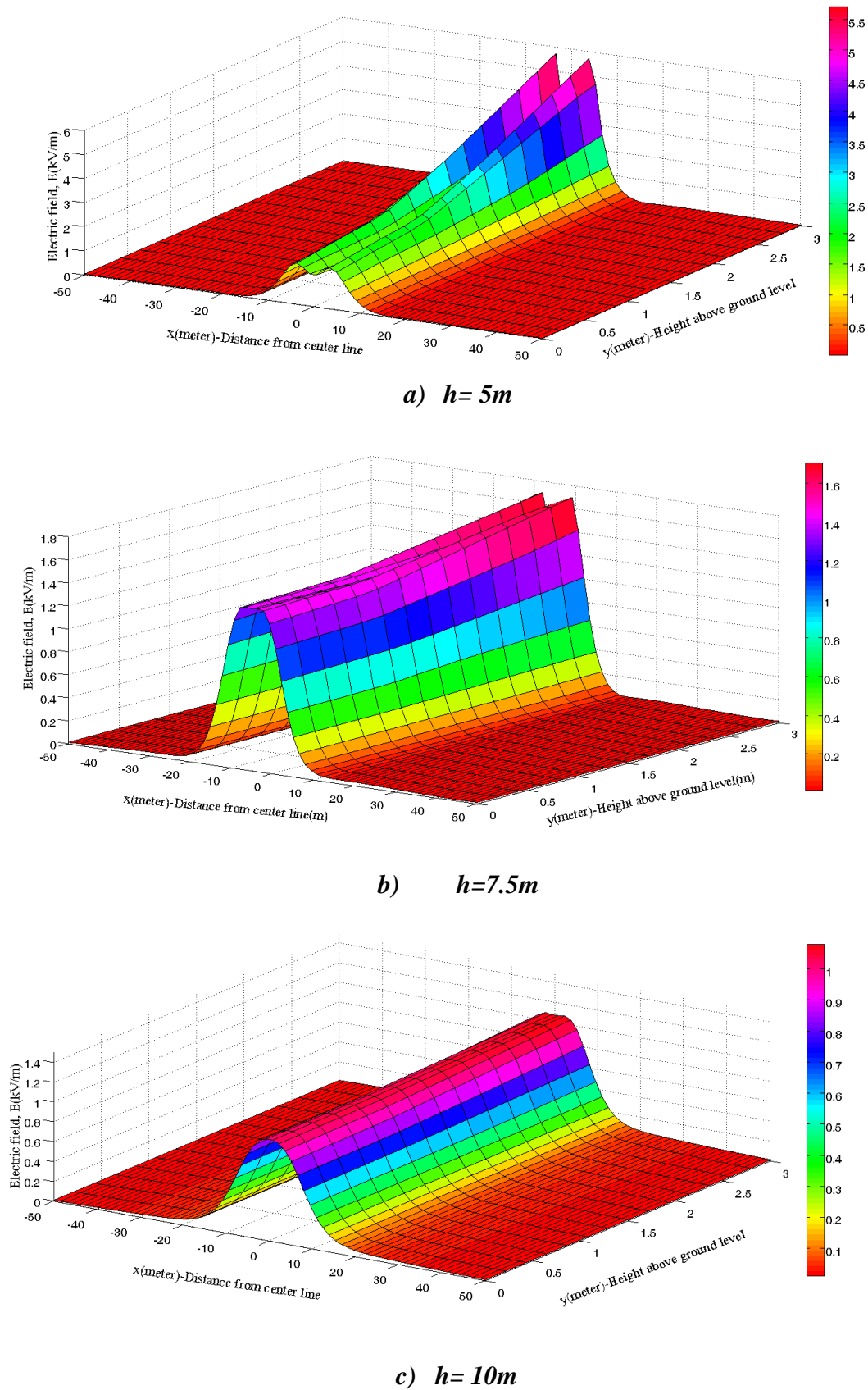
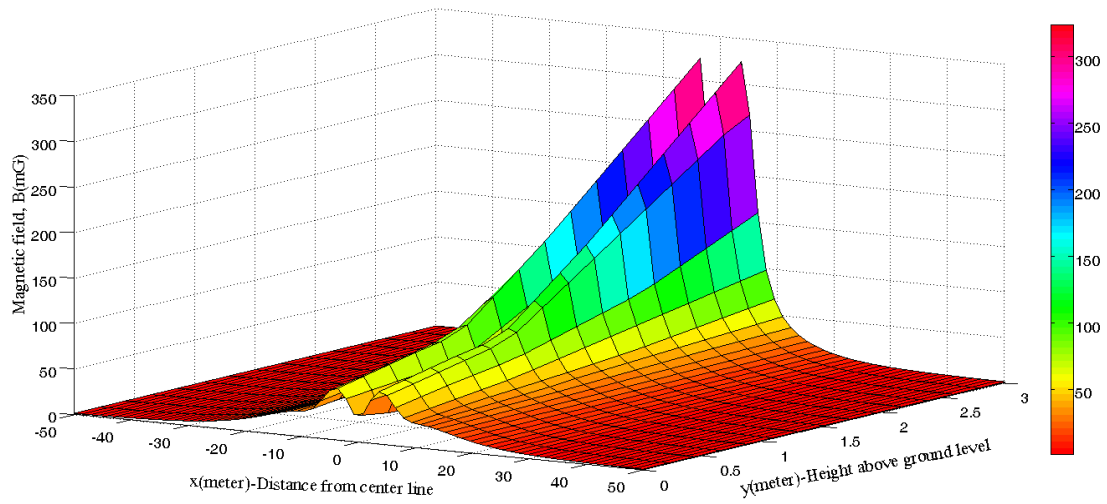
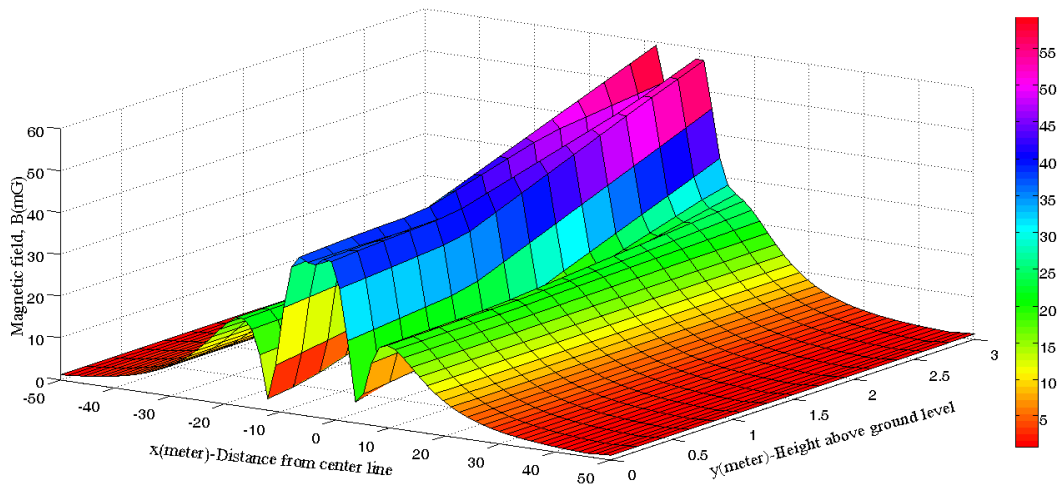


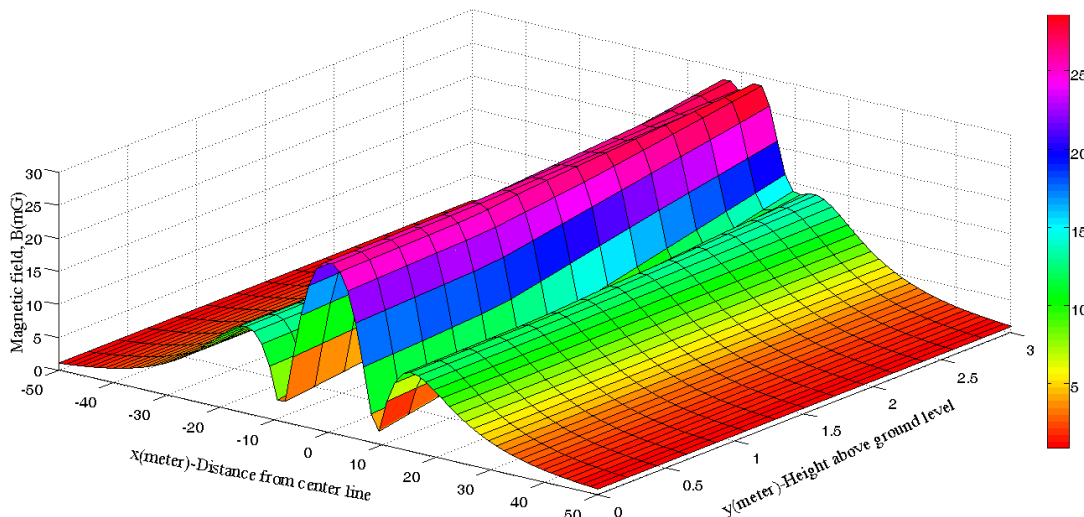
Figure (6) Distribution of the electric field as a function of the node's x, y coordinates at three span locations (h) crossing of public services.



a) $h=5m$



b) $h=7.5$



c) $h=10m$

Figure (7) Distribution of the magnetic field as a function of the node's x, y coordinates at three span locations (h) crossing of public services.

The performance of the ANFIS is tested in the second geometry, for which ANFIS is not trained. The corresponding FEM solution is also obtained in order to compare the ANFIS results. The new geometry is rearrange for the conductors configuration, where flat (horizontal) configuration is considered at span location ($h=5m$) crossing structures.

Table 2 summarized test results for several new configuration cases where E and B calculations by the ANFIS and the FEM have been compared.

Table 2: Intensity electric field and magnetic field for flat conductors configuration case of the examined electromagnetic field problem, obtained by the FEM and ANFIS

Coordinates		FEM		ANFIS		$e_E(\%)$	$e_B(\%)$
$x(m)$	$y(m)$	$E(kV/m)$	$B(mG)$	$E(kV/m)$	$B(mG)$		
1	1.5	6.3043	510.8300	6.1316	496.0659	2.7393	2.8902
3	0.25	2.3883	222.6600	2.4417	223.7100	2.2351	0.4716
13	0	0.8723	66.2820	0.8819	66.6666	1.1009	0.5803
15	0.5	0.5367	40.1160	0.5409	40.4319	0.7895	0.7876
19	2	0.2283	17.7490	0.2297	17.8528	0.6058	0.5848
25	2.25	0.0860	6.8794	0.0863	6.9029	0.3555	0.3413
35	3	0.0508	2.1753	0.0510	2.1793	0.2695	0.1826

For this case, the average absolute error between FEM and ANFIS is 0.5396% and 0.4353% for the examined electric field and magnetic field problems respectively. Figure 8 and Figure 9 show horizontal profile of electric field and magnetic field as a function of the node's coordinate x in the air for the new case (flat configuration), as it is calculated by FEM and ANFIS. In both cases, it is clear that ANFIS seems to follow satisfactory the results of FEM.

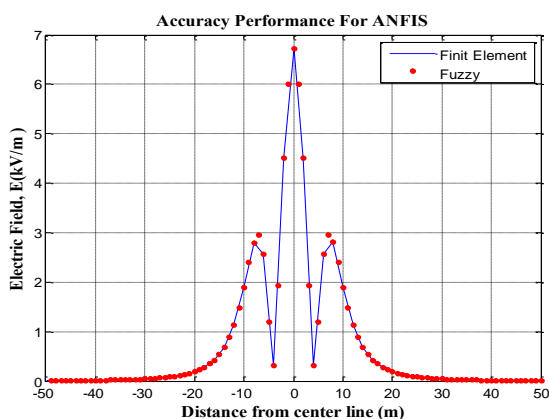


Figure (8) Electric field values on Horizontal profile of the flat configuration calculations by FEM and ANFIS

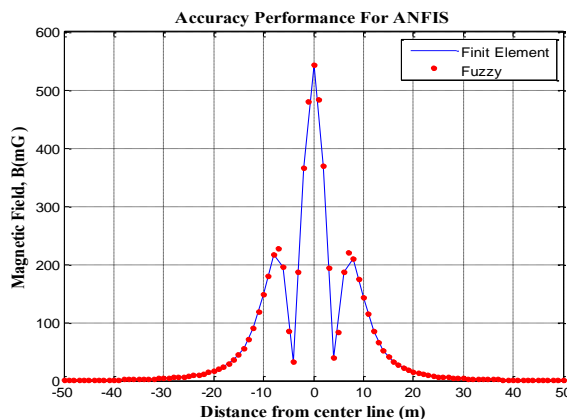


Figure (9) Magnetic field values on Horizontal profile of the flat configuration calculations by FEM and ANFIS

Three-dimensional distribution of the electric and magnetic fields in obtained by the ANFIS is shown in Figure 10 and Figure 11 for the span location at $h=5m$ crossing structures or building .

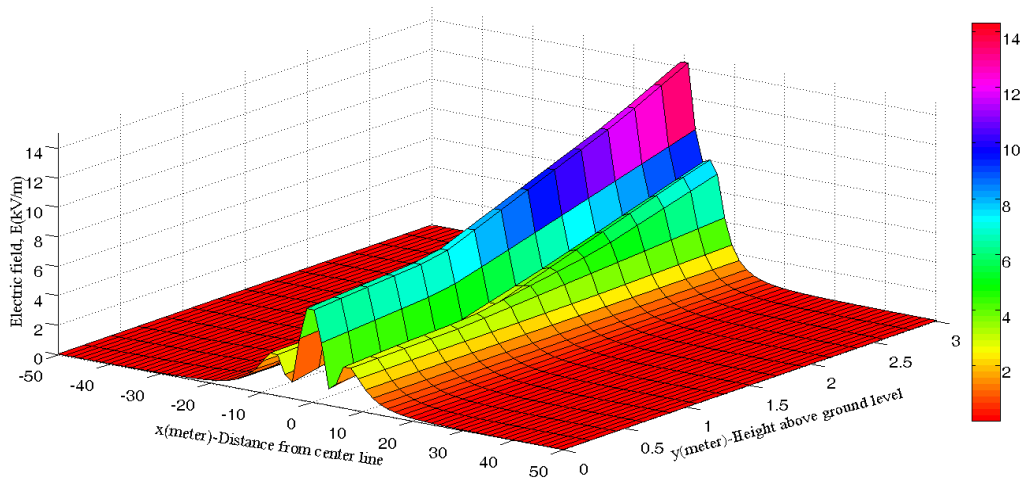


Figure (10) Distribution of the electric field as a function of the node's x, y coordinates

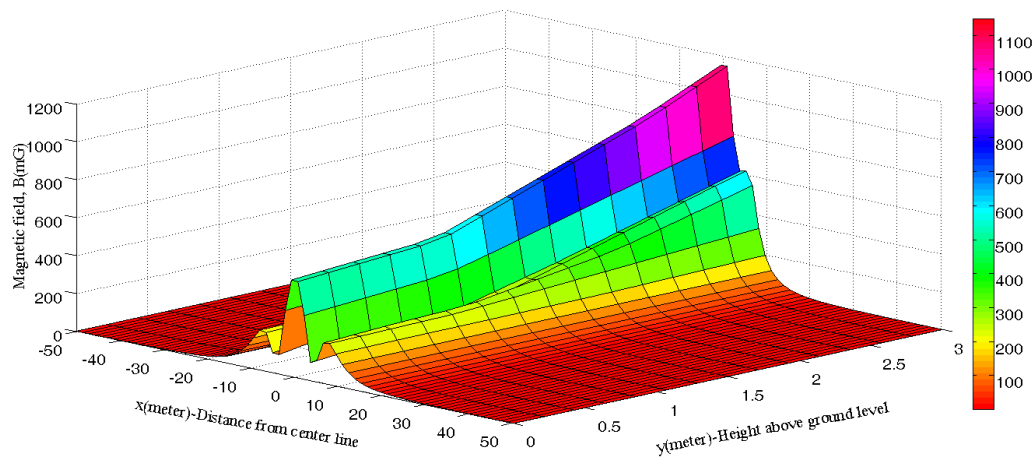


Figure (11) Distribution of the magnetic field as a function of the node's x, y coordinates

5. Conclusion

In this research, ANFIS may be used for estimation the electric and magnetic fields around an Iraqi 132kV overhead power transmission line. A suitable ANFIS model has been developed and trained in some configuration cases of this problem. In this research, ANFIS performance has been tested for many configuration cases, differing significantly from the cases used for training. From the test results it could be concluded that, results of the simulations presented in this research show that the application of the ANFIS to electromagnetic field approximation gives satisfactory results. ANFIS test are in a very good agreement with the results obtained by FEM. Maximal absolute error is less than 4%.

6. References

- [1] J. Weiss and Z. Csendes, "A one-step finite element method for multiconductor skin effect problems," IEEE Trans. Power Appart. Syst., vol. PAS-101, no. 10, pp. 3796-3803, Oct. 1982.
- [2] D. Labridis and P. Dokopoulos, "Finite element computation of field, losses and forces in a three-phase gas cable with nonsymmetrical conductor arrangement," IEEE Trans. Power Delivery, vol. PWDR-3, pp. 1326-1333, Oct. 1988
- [3] I. G. Damouis, K. J. Satsios, D. P. Labridis, P. S. Dokopoulos, "A fuzzy logic system for calculation of the interference of overhead transmission lines on buried pipelines", Electric Power Systems Research, vol. 57, pp. 105-113, 2001.
- [4] I. G. Damouis, K. J. Satsios, D. P. Labridis, P. S. Dokopoulos, "Combined fuzzy logic and genetic algorithm techniques-application to an electromagnetic field problem", Fuzzy sets and systems, vol. 129, pp. 371-386, 2002.
- [5] T. I. Maris, L. Ekonomou, G. P. Fotis, A. Nakulas, E. Zoulias, "Electromagnetic field identification using artificial neural networks" , Proc. of the 8th Conference on 8th WSEAS International Conference on Neural Networks - Volume 8 , Canada, pp.84-89, 2007.
- [6] G. Capizzi, G., S. Coco, A. Laudani, "A Neural Network tool for the prediction of electromagnetic field in urban environment", Proc. of the 12th Biennial IEEE Conference on Electromagnetic Field Computation, pp. 60, 2006
- [7] J.-S. R. Jang, "ANFIS: Adaptive-Neural-Based Fuzzy Inference Systems", IEEE Transactions on Systems, Man, and Cybernetics, Vol. 23, No. 3, pp. 665-685, 1993.
- [8] R. G. Olsen and P. S. Wong, "Characteristics of Low Frequency Electric and Magnetic Fields in the Vicinity of Electric Power Lines", IEEE Trans. on Power Delivery, Vol. 7, No. 4, pp. 2046-2055 , 1992.
- [9] S. Reitzinger, U. Schreiber, and U. V. Rienen, "Electro-quasi-static calculation of electric field strength on high-voltage insulators with an algebraic multigrid algorithm," IEEE Trans. Magn., vol. 39, pp. 2129-2132, 2003.
- [10] Hasselgren L., Moller E., Hamnerius Y., "Calculation of Magnetic Shielding of a Substation at Power Frequency Using FEM", IEEE Transactions on Power Delivery, Vol. 9, No. 3, 1994.
- [11] Ministry of Electricity, Iraq, "Iraq Super Grid Projects 132 kV Single and Double Circuit Steel Tower Transmission Lines", Volume 1 Technical Specification, 2006.
- [12] G.B. Iyyuni and S.A. Sebo, "Study of Transmission Line Magnetic Fields," Proceedings of the Twenty-Second Annual North American, IEEE Power Symposium, pp.222-231, 1990.
- [13] R. Jang, "Input selection for ANFIS learning," in Proc. 5th IEEE Int. Conf. Fuzzy Systems, Sep. 8-11, 1996, vol. 2, pp. 1493-1499.